Published in final edited form as:
J Mol Biol. 2009 October 16; 393(1): 1–9. doi:10.1016/j.jmb.2009.07.091.

Crystal Structure of the Frizzled-like Cysteine-rich Domain of the Receptor Tyrosine Kinase MuSK

Amy L. Stiegler[1,2,§], **Steven J. Burden**[2], and **Stevan R. Hubbard**[1,*]

[1]Department of Pharmacology and Structural Biology, Programs, Kimmel Center for Biology and Medicine of the Skirball Institute, New York University School of Medicine, New York, NY 10016

[2]Molecular Neurobiology Programs, Kimmel Center for Biology and Medicine of the Skirball Institute, New York University School of Medicine, New York, NY 10016

Abstract

Muscle-specific kinase (MuSK) is an essential receptor tyrosine kinase for establishment and maintenance of the neuromuscular junction (NMJ). Activation of MuSK by agrin, a neuronally derived heparan-sulfate proteoglycan, and LRP4, the agrin receptor, leads to clustering of acetylcholine receptors on the postsynaptic side of the NMJ. The ectodomain of MuSK comprises three immunoglobulin-like domains and a cysteine-rich domain (Fz-CRD) related to those in Frizzled proteins, the receptors for Wnts. Here, we report the crystal structure of the MuSK Fz-CRD at 2.1 Å resolution. The structure reveals a five disulfide-bridged domain similar to CRDs of Frizzled proteins, but with a divergent C-terminal region. An asymmetric dimer present in the crystal structure implicates surface hydrophobic residues that may function in homotypic or heterotypic interactions to mediate co-clustering of MuSK, rapsyn, and acetylcholine receptors at the NMJ.

Keywords

crystal structure; Frizzled; MuSK; neuromuscular junction; receptor tyrosine kinase

Formation of the vertebrate neuromuscular junction (NMJ) requires a complex exchange of signals between innervating motor neurons and muscle cells, resulting in a highly specialized postsynaptic membrane and a differentiated nerve terminal.[1] The receptor tyrosine kinase (RTK) MuSK (muscle-specific kinase) is essential for prepattering acetylcholine receptors (AChRs) in muscle prior to innervation and for agrin-induced AChR clustering during formation of the NMJ. Mice lacking MuSK fail to establish muscle prepatterning, are devoid of functional NMJs, and die at birth due to a failure to breathe.[2,3] Agrin, a neurally derived heparan-sulfate proteoglycan, activates MuSK and stabilizes nascent NMJs by binding to LRP4 (low-density lipoprotein receptor-related protein-4), which forms a complex with MuSK.[4,5]

*Corresponding author: Dr. Stevan R. Hubbard Skirball Institute of Biomolecular Medicine New York University School of Medicine New York, NY 10016 phone (212) 263-8938 fax (212) 263-8951 stevan.hubbard@med.nyu.edu.
§Present address: Department of Pharmacology Yale University School of Medicine 333 Cedar Street, SHM B-302 New Haven, CT 06520

Accession Numbers
The coordinates and structure factors for MuSK-CRD were deposited in the Protein Data Bank with accession number 3HKL.

Impairment in the establishment or maintenance of AChR clusters, or defects in the function of AChRs, is associated with disorders in neuromuscular transmission, including myasthenia gravis and congenital myasthenic syndromes (CMS).[6,7]

MuSK comprises three immunoglobulin (Ig)-like domains, a cysteine-rich domain (CRD) related to that of the Wnt-receptor Frizzled, a transmembrane helix, and a cytoplasmic tyrosine kinase domain (Figure 1(a)). The first and second Ig-like domains of MuSK (Ig1-2) are crucial for agrin-induced MuSK activation,[8] and we previously reported the crystal structure of MuSK Ig1-2.[9] This structure showed that Ig1-2 are configured in a linear, semi-rigid arrangement, and revealed hydrophobic residues on the surface of Ig1 that are required for activation of MuSK by agrin.

The MuSK CRD was originally classified as a C6 box plus an additional Ig-like domain (Ig4).[10,11] It was subsequently identified as a Frizzled-like CRD (Fz-CRD), defined by ten cysteine residues forming five disulfide bonds,[12,13] although the MuSK Fz-CRD shares less than 20% sequence identity with Frizzled CRDs. Frizzled proteins are seven-pass transmembrane receptors that bind members of the Wnt family of secreted glycoproteins via their extracellular CRDs.[14,15] In addition to MuSK, Fz-CRDs are present in the non-Frizzled proteins smoothened,[16] carboxypeptidase Z,[17] and the RTKs Ror1 and Ror2.[12,13]

The role of the Fz-CRD in MuSK was partially addressed through deletion studies, in which full-length MuSK lacking the Fz-CRD was expressed in $MuSK^{-/-}$ myotubes. These studies showed that the Fz-CRD is dispensable for agrin-induced MuSK activation and AChR clustering, but that its absence affects the ability of MuSK to co-cluster with rapsyn and AChRs.[8] Therefore, the MuSK Fz-CRD might mediate a direct interaction between MuSK and AChR on the cell surface or could bind to an unknown transmembrane protein—the so-called RATL (rapsyn-associated transmembrane linker)[18]—to bridge MuSK and cytoplasmic rapsyn. Whether the Fz-CRD in mammalian MuSK acts solely as a structural scaffold for MuSK-rapsyn-AChR co-clustering, or whether it regulates co-clustering by binding a Wnt or another secreted ligand, is not known.

Structure of MuSK Fz-CRD

To obtain insights into the function of the Fz-CRD in mammalian MuSK (also referred to as MuSK-CRD in the following), we have determined the crystal structure of rat MuSK-CRD at 2.1 Å resolution. Data collection and refinement statistics are given in Table 1. The crystal structure reveals that MuSK-CRD adopts the mainly α-helical fold observed for the CRDs of Frizzled-8 (Fz8-CRD) and secreted Frizzled-related protein-3 (sFRP3-CRD),[19] with the ten cysteine residues incorporated into the same five disulfide bonds (Figure 1(b)). There are two short N-terminal β strands (β1 and β2) and either three (α1, α3, and α4) or four (plus α5) α helices in the two copies of MuSK-CRD in the asymmetric unit.

For the majority of the MuSK-CRD structure (residues 314-409), the two copies in the asymmetric unit superimpose well, with a root-mean-square deviation of 1.1 Å for 96 Cα positions. However, in the C-terminal half of the domain, between residues 410 and 431, the two copies diverge significantly (Figure 1(c)). In one MuSK-CRD molecule (copy A), this region contains an α helix (α5, residues 410-423), while in the second molecule (copy B), this segment is coil-like, and residues 421-428 interact with residues in copy A (see below).

The two MuSK-CRDs in the asymmetric unit are packed as an asymmetric (non-two-fold-related) dimer whose interface is predominantly hydrophobic (Figures 2(a) and 2(b)). The interface buries 1,633 $Å^2$ of total surface area (next largest interface in the crystal is 890 $Å^2$), has a shape complementarity (sc) value of 0.74,[20] and a PISA complex significance score (CSS) of 1.0.[21] These interface metrics are consistent with biologically relevant protein-protein

interactions. The principal contacts are made by Leu365, Tyr397, Leu404, Phe405, and Tyr452 from one MuSK-CRD molecule (copy A), and Tyr341, Pro342, Ala347, Leu350, Leu351, Tyr422, and Phe428 from the second molecule (copy B) (Figure 2(b)). These residues are well conserved in MuSK across species, but are not conserved in Frizzled CRDs nor in Ror1 and Ror2 (Figure 3(a)).

Formation of this asymmetric dimer is contingent upon the absence of α5 in copy B of MuSK-CRD; an intact α5 in copy B would sterically clash with copy A (Figure 2(c)). Two glycines in α5 (Gly415 and Gly420) are likely responsible for the quasi-stability of this helix. Gly420 is conserved in all MuSK species, whereas Gly415 in rat and mouse MuSK is a glutamic acid in human and other primates, chick, and zebrafish (Figure 3(a)). In the crystal lattice, α5 is packed against another A-type (α5-containing) MuSK-CRD along the $P2_1$ screw axis, suggesting a possible mode of MuSK self-association on the cell surface.

Although the isolated MuSK Fz-CRD behaves as a monomer in solution, as judged by size-exclusion chromatography (loading concentration up to ~1 mM) and static multi-angle light scattering (data not shown), the Fz-CRD in full-length MuSK is approximately 40 residues N-terminal of the transmembrane helix, which, through reduction in dimensionality (from three to quasi-two dimensions), could significantly enhance the dimerization propensity of the Fz-CRD. A MuSK Fz-CRD homotypic interaction at the cell surface could potentially contribute to stabilization of either an inactive or active dimeric form of MuSK (with respect to the disposition of the cytoplasmic kinase domains). With regard to the Ig1-mediated dimer observed in the Ig1-2 crystal structure,[9] based on the presumed linearity of the three Ig-like domains, the Fz-CRD dimer would likely bridge two such dimers (*trans*, resulting in higher-order oligomerization) rather than contributing to the Ig1-mediated dimer (*cis*).

N-linked glycosylation

Two N-linked glycosylation sites are present in MuSK-CRD,[22] Asn338 and Asn459. Recombinant MuSK-CRD purified from insect cells, with a calculated molecular weight (protein) of 22 kDa, migrates on SDS-PAGE as a diffuse band of apparent molecular weight ~30 kDa. Treatment of MuSK-CRD with endoglycosidase F results in faster migration (data not shown), supporting the conclusion that MuSK-CRD as expressed in insect cells is glycosylated. Glycoproteins expressed in insect cells typically contain high-mannose N-glycans of the form $(Man)_nGlcNAc_2$. In the crystal structure of MuSK-CRD, electron density for two N-acetylglucosamine (NAG/GlcNAc) groups are visible at Asn338 (end of β2) in both copies of MuSK-CRD. The C6 hydroxyl group of the first NAG on Asn338 in copy B makes two contacts (Figure 2(d)): one intramolecular hydrogen bond with the side chain of Tyr341 (copy B), and one intermolecular hydrogen bond with the side chain of Glu403 (copy A). Glu403 is also hydrogen-bonded to the C2 acetamido nitrogen of the second NAG. Thus, the intermolecular carbohydrate interactions mediated by Glu403 could contribute to stabilization of the MuSK-CRD asymmetric dimer. Asn338 and Glu403 are conserved in other MuSK species including *Torpedo californica* (Figure 3(a)). Glycosylated Asn459 is located in a variably spliced insert in the C-terminal region, beyond the last cysteine of the domain, and in the crystal structure is disordered in both MuSK-CRD copies.

Comparison with Frizzled CRDs

Despite the similarity in the overall folds of MuSK-CRD and Fz8-CRD—root-mean-square deviation (r.m.s.d.) of 1.4 Å in the ten cysteine Cα positions—there are significant structural deviations which lead to an r.m.s.d. of 3.1 Å over 111 Cα positions (Figure 3(b)). The major deviation is found in the C-terminal half of the domain, where an 11-residue insertion in MuSK-CRD relative to Fz8/sFRP3-CRD forms the aforementioned α5 in copy A (Figures 3(a) and 3(b)). In copy B of MuSK-CRD, the conformation of this region is also divergent from that in

Fz8/sFRP3-CRD (necessarily, because of the large insertion). Other differences in structure are found in the β2-α1 loop and in α1 (Figure 3(b)). Instead of the two relatively short helices α1 and α2 in Frizzled CRDs, there is a single extended helix (α1) in MuSK-CRD.

Another unique structural feature of MuSK-CRD is a one-residue insertion at the end of α4. In Fz8/sFRP3-CRD, α4 starts before the seventh disulfide-bridged cysteine (Cys80) and extends beyond the eighth cysteine (Cys91) (Figure 3(b)), whereas in MuSK-CRD, there is a one-residue insertion, Leu404, prior to the eighth cysteine (Cys406) (Figure 3(a)). This insertion creates a bulge in α4 (technically terminating the helix), exposing to solvent Leu404 and Phe405 (Figure 3(b)), which (in copy A) are situated in the asymmetric dimer interface (Figure 2(b)). Leu404 is conserved in all species of MuSK, and Phe405 is either phenylalanine or tyrosine. This one-residue insertion is present as well in the Fz-CRDs of the RTKs Ror1 and Ror2 (Figure 3(a)).

In the crystal structures of Fz8- and sFRP3-CRD, a non-crystallographic dimer (symmetric) is present, which, in both cases, is mediated by residues in the α3-α4 loop and in the C-terminal segment.[19] These residues do not overlap with those that constitute the MuSK-CRD asymmetric dimer interface (Figure 3(c)). Fz8- and sFRP3-CRD are also monomeric in solution, yet the semi-conserved dimerization interface suggests that they may form homo- or heterodimers on the cell surface.[19] This hypothesis is supported by the observation that *Xenopus laevis* Frizzled-3 forms CRD-dependent homodimers.[23] Furthermore, interactions between the Fz-CRD of Ror2 and the CRDs of Frizzled-2 and Frizzled-5 were observed by coimmunoprecipitation, suggesting that Fz-CRDs may heterodimerize to elicit specific responses.[24]

Wnt binding

Several studies have suggested potential roles for Wnt signaling in NMJ formation. However, canonical Wnt signaling through β-catenin has largely been discounted, as TCF/LEF-induced transcriptional upregulation has not been correlated with NMJ formation.[25,26] A recent study indicates that Wnt3 in chick potentiates agrin-induced AChR clustering through non-canonical Wnt signaling involving the small GTPases Rac1 and RhoA.[27] However, whether Wnt3 acts through MuSK or a Frizzled protein was not addressed. In zebrafish, the interaction between Wnt11r and the Fz-CRD of MuSK/Unplugged was shown to be critical for AChR prepatterning.[28] Also relevant to Wnt-RTK interactions, Wnt3a and Wnt5a bind to the Fz-CRD of Ror2 to mediate cell polarization and migration.[24,29,30]

The crystal structure of mouse Fz8-CRD permitted a detailed structure-function analysis of Wnt binding.[19] From these studies, it was concluded that the binding site for Wnt8 involves residues in the β1-β2 loop, the α3-α4 loop, and the C-terminal tail. The structure-based sequence alignment of the MuSK and Frizzled-8 CRDs suggests that the MuSK Fz-CRD is unlikely to bind Wnt8, due to lack of sequence conservation in these regions (Figure 3(a)). Interestingly, the Fz-CRDs of RTKs that have been confirmed as Wnt binders (zebrafish MuSK, Ror1, and Ror2) all contain a Kringle domain (three disulfide-bonded CRD) just C-terminal to the Fz-CRD. Athough there is no evidence that the Kringle domain is necessary for Wnt binding, mammalian MuSK proteins lack this domain.

Because LRP5 and LRP6 act as co-receptors of Wnts along with Frizzled proteins,[31] it is conceivable that LRP4, in addition to functioning as the agrin receptor,[4,5] could serve in muscle as a Wnt co-receptor. In the zebrafish study,[28] whether Wnt11r interacts with LRP4 as well as with MuSK/Unplugged was not tested.

Summary

The high-resolution crystal structure of the MuSK Fz-CRD provides a molecular basis for further functional studies of this domain, leading to a broader understanding of the complex signaling events downstream of MuSK that mediate clustering of AChRs at the NMJ. Several potential roles of the MuSK Fz-CRD include MuSK oligomerization, MuSK-RATL-rapsyn association, and Wnt binding. Additional cell biological and biochemical studies will be required to distinguish between these possibilities.

Acknowledgments

We thank L. Cunha for the SEC-MALS analysis, J. Wu for help in x-ray data collection, and J. Burrill for technical support. Financial support is acknowledged from the NIH (R01 NS053414 to S.R.H., R01 NS036193 to S.J.B.). A.L.S. was partially supported by NIH/NIGMS training grant T32 GM066704.

References

1. Burden SJ. Building the vertebrate neuromuscular synapse. J. Neurobiol 2002;53:501–511. [PubMed: 12436415]
2. Gautam M, Noakes PG, Moscoso L, Rupp F, Scheller RH, Merlie JP, Sanes JR. Defective neuromuscular synaptogenesis in agrin-deficient mutant mice. Cell 1996;85:525–535. [PubMed: 8653788]
3. DeChiara TM, Bowen DC, Valenzuela DM, Simmons MV, Poueymirou WT, Thomas S, Kinetz E, Compton DL, Rojas E, Park JS, Smith C, DiStefano PS, Glass DJ, Burden SJ, Yancopoulos GD. The receptor tyrosine kinase MuSK is required for neuromuscular junction formation in vivo. Cell 1996;85:501–512. [PubMed: 8653786]
4. Glass DJ, Bowen DC, Stitt TN, Radziejewski C, Bruno J, Ryan TE, Gies DR, Shah S, Mattsson K, Burden SJ, DiStefano PS, Valenzuela DM, DeChiara TM, Yancopoulos GD. Agrin acts via a MuSK receptor complex. Cell 1996;85:513–523. [PubMed: 8653787]
5. Kim N, Stiegler AL, Cameron TO, Hallock PT, Gomez AM, Huang JH, Hubbard SR, Dustin ML, Burden SJ. Lrp4 is a receptor for Agrin and forms a complex with MuSK. Cell 2008;135:334–42. [PubMed: 18848351]
6. Engel AG, Sine SM. Current understanding of congenital myasthenic syndromes. Curr. Opin. Pharmacol 2005;5:308–21. [PubMed: 15907919]
7. Beeson D, Webster R, Cossins J, Lashley D, Spearman H, Maxwell S, Slater CR, Newsom-Davis J, Palace J, Vincent A. Congenital myasthenic syndromes and the formation of the neuromuscular junction. Ann. NY Acad. Sci 2008;1132:99–103. [PubMed: 18567858]
8. Zhou H, Glass DJ, Yancopoulos GD, Sanes JR. Distinct domains of MuSK mediate its abilities to induce and to associate with postsynaptic specializations. J. Cell Biol 1999;146:1133–1146. [PubMed: 10477765]
9. Stiegler AL, Burden SJ, Hubbard SR. Crystal structure of the agrin-responsive immunoglobulin-like domains 1 and 2 of the receptor tyrosine kinase MuSK. J. Mol. Biol 2006;364:424–33. [PubMed: 17011580]
10. Jennings CG, Dyer SM, Burden SJ. Muscle-specific trk-related receptor with a kringle domain defines a distinct class of receptor tyrosine kinases. Proc. Natl. Acad. Sci. U.S.A 1993;90:2895–2899. [PubMed: 8385349]
11. Valenzuela DM, Stitt TN, DiStefano PS, Rojas E, Mattsson K, Compton DL, Nunez L, Park JS, Stark JL, Gies DR, Thomas S, Le Beau MM, Fernald AA, Copeland NG, Jenkins NA, Burden SJ, Glass DJ, Yancopoulos GD. Receptor tyrosine kinase specific for the skeletal muscle lineage: expression in embryonic muscle, at the neuromuscular junction, and after injury. Neuron 1995;15:573–584. [PubMed: 7546737]
12. Xu YK, Nusse R. The Frizzled CRD domain is conserved in diverse proteins including several receptor tyrosine kinases. Curr Biol 1998;8:R405–6. [PubMed: 9637908]
13. Masiakowski P, Yancopoulos GD. The Wnt receptor CRD domain is also found in MuSK and related orphan receptor tyrosine kinases. Curr. Biol 1998;8:R407. [PubMed: 9637909]

14. Vinson CR, Conover S, Adler PN. A Drosophila tissue polarity locus encodes a protein containing seven potential transmembrane domains. Nature 1989;338:263–4. [PubMed: 2493583]
15. Bhanot P, Brink M, Samos CH, Hsieh JC, Wang Y, Macke JP, Andrew D, Nathans J, Nusse R. A new member of the frizzled family from Drosophila functions as a Wingless receptor. Nature 1996;382:225–30. [PubMed: 8717036]
16. Alcedo J, Ayzenzon M, Von Ohlen T, Noll M, Hooper JE. The Drosophila smoothened gene encodes a seven-pass membrane protein, a putative receptor for the hedgehog signal. Cell 1996;86:221–32. [PubMed: 8706127]
17. Song L, Fricker LD. Cloning and expression of human carboxypeptidase Z, a novel metallocarboxypeptidase. J. Biol. Chem 1997;272:10543–50. [PubMed: 9099699]
18. Apel ED, Glass DJ, Moscoso LM, Yancopoulos GD, Sanes JR. Rapsyn is required for MuSK signaling and recruits synaptic components to a MuSK-containing scaffold. Neuron 1997;18:623–635. [PubMed: 9136771]
19. Dann CE, Hsieh JC, Rattner A, Sharma D, Nathans J, Leahy DJ. Insights into Wnt binding and signalling from the structures of two Frizzled cysteine-rich domains. Nature 2001;412:86–90. [PubMed: 11452312]
20. Lawrence MC, Colman PM. Shape complementarity at protein/protein interfaces. J. Mol. Biol 1993;234:946–950. [PubMed: 8263940]
21. Krissinel E, Henrick K. Inference of macromolecular assemblies from crystalline state. J. Mol. Biol 2007;372:774–97. [PubMed: 17681537]
22. Watty A, Burden SJ. MuSK glycosylation restrains MuSK activation and acetylcholine receptor clustering. J. Biol. Chem 2002;277:50457–62. [PubMed: 12399462]
23. Carron C, Pascal A, Djiane A, Boucaut JC, Shi DL, Umbhauer M. Frizzled receptor dimerization is sufficient to activate the Wnt/beta-catenin pathway. J. Cell Sci 2003;116:2541–50. [PubMed: 12734397]
24. Oishi I, Suzuki H, Onishi N, Takada R, Kani S, Ohkawara B, Koshida I, Suzuki K, Yamada G, Schwabe GC, Mundlos S, Shibuya H, Takada S, Minami Y. The receptor tyrosine kinase Ror2 is involved in non-canonical Wnt5a/JNK signalling pathway. Genes Cells 2003;8:645–54. [PubMed: 12839624]
25. Luo ZG, Wang Q, Zhou JZ, Wang J, Luo Z, Liu M, He X, Wynshaw-Boris A, Xiong WC, Lu B, Mei L. Regulation of AChR clustering by Dishevelled interacting with MuSK and PAK1. Neuron 2002;35:489–505. [PubMed: 12165471]
26. Zhang B, Luo S, Dong XP, Zhang X, Liu C, Luo Z, Xiong WC, Mei L. Beta-catenin regulates acetylcholine receptor clustering in muscle cells through interaction with rapsyn. J. Neurosci 2007;27:3968–73. [PubMed: 17428970]
27. Henriquez JP, Webb A, Bence M, Bildsoe H, Sahores M, Hughes SM, Salinas PC. Wnt signaling promotes AChR aggregation at the neuromuscular synapse in collaboration with agrin. Proc. Natl. Acad. Sci. U.S.A 2008;105:18812–7. [PubMed: 19020093]
28. Jing L, Lefebvre JL, Gordon LR, Granato M. Wnt signals organize synaptic prepattern and axon guidance through the zebrafish unplugged/MuSK receptor. Neuron 2009;61:721–33. [PubMed: 19285469]
29. Nishita M, Yoo SK, Nomachi A, Kani S, Sougawa N, Ohta Y, Takada S, Kikuchi A, Minami Y. Filopodia formation mediated by receptor tyrosine kinase Ror2 is required for Wnt5a-induced cell migration. J. Cell Biol 2006;175:555–62. [PubMed: 17101698]
30. Liu Y, Rubin B, Bodine PV, Billiard J. Wnt5a induces homodimerization and activation of Ror2 receptor tyrosine kinase. J. Cell. Biochem 2008;105:497–502. [PubMed: 18615587]
31. He X, Semenov M, Tamai K, Zeng X. LDL receptor-related proteins 5 and 6 in Wnt/beta-catenin signaling: arrows point the way. Development 2004;131:1663–77. [PubMed: 15084453]
32. Terwilliger TC, Berendzen J. Automated MAD and MIR structure solution. Acta Crystallogr. D 1999;55:849–861. [PubMed: 10089316]
33. Vagin AA, Teplyakov A. MOLREP: an automated program for molecular replacement. J. Appl. Cryst 1997;30:1022–1025.
34. Perrakis A, Morris R, Lamzin VS. Automated protein model building combined with iterative structure refinement. Nat. Struct. Biol 1999;6:458–63. [PubMed: 10331874]

35. Emsley P, Cowtan K. Coot: model-building tools for molecular graphics. Acta Crystallogr. D 2004;60:2126–2132. [PubMed: 15572765]

36. Murshudov GN, Vagin AA, Dodson EJ. Refinement of macromolecular structures by the maximum-likelihood method. Acta Crystallogr. D 1997;53:240–255. [PubMed: 15299926]

37. Laskowski RA, MacArthur MW, Moss DS, Thornton JM. PROCHECK: a program to check the stereochemical quality of protein structures. J. Appl. Cryst 1993;26:283–291.

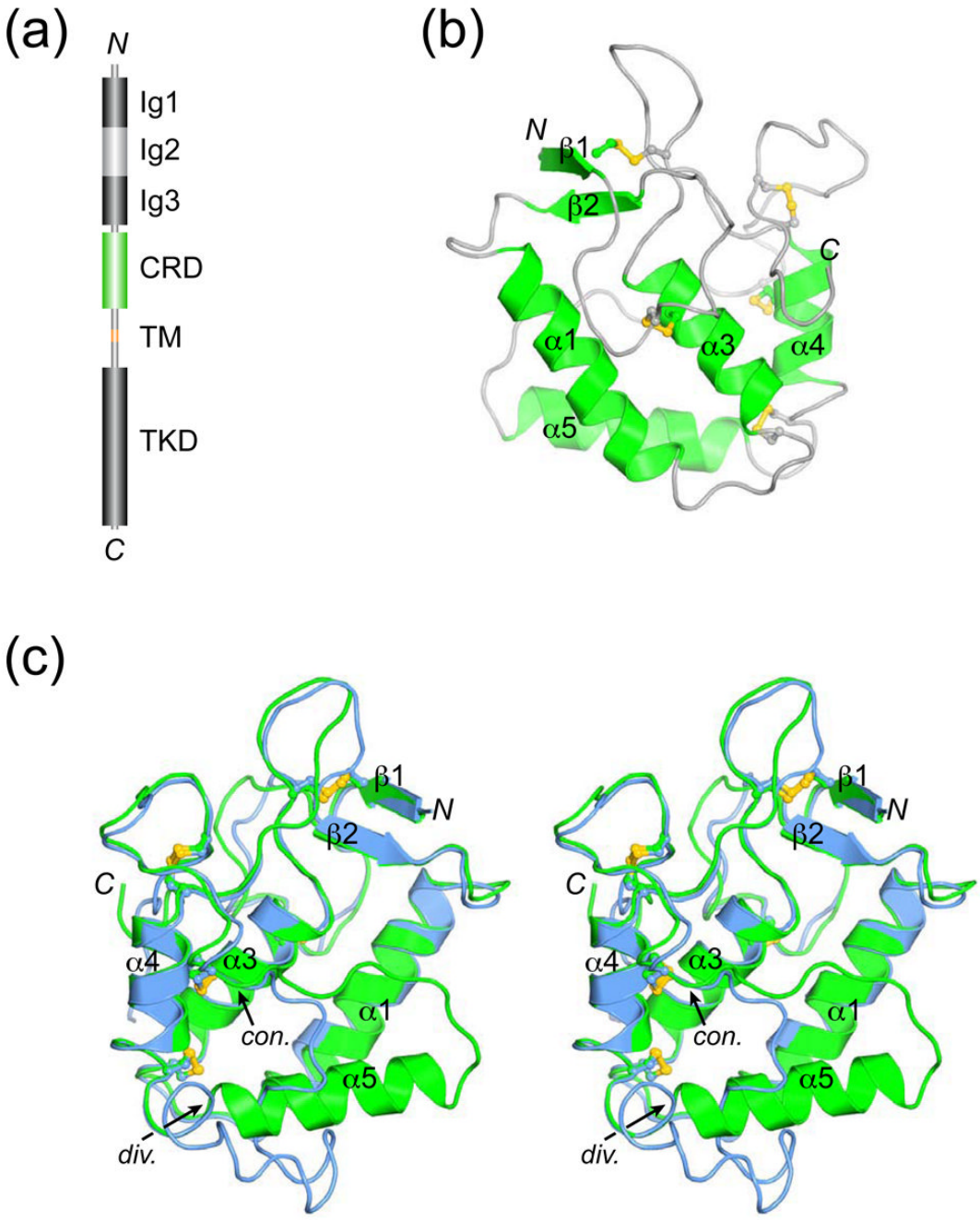

Figure 1.

Crystal structure of MuSK-CRD. (a) Schematic diagram of mammalian MuSK (human, 869 residues) drawn to linear scale. Ig1-3, immunoglobulin-like domains; CRD, cysteine-rich domain; TM, transmembrane helix; TKD, tyrosine kinase domain. (b) Ribbon diagram of MuSK-CRD. The secondary structural elements are labeled according to Dann et al.[19] Accordingly, α1 is extended in MuSK-CRD relative to α1 in Fz8-CRD (PDB code 1IJY)[19] and there is no α2. Cysteine side chains are shown in ball-and-stick representation, and the sulfur atoms are colored yellow. The N- and C-termini are labeled *N* and *C*, respectively. (c) Stereo view of a superposition of the two copies of MuSK-CRD in the asymmetric unit. Copies A and B are colored green and blue, respectively. The orientation is approximately 180° from that in

(b), rotated about a vertical axis in the plane of the figure. The arrows indicate where in the C-terminal half of the molecules the two copies diverge (*div.*) and converge (*con.*). Figures 1 and 3 were rendered with PyMOL (http://pymol.sourceforge.net). The MuSK-CRD structure was determined by single anomalous diffraction (SAD) phasing using SOLVE.[32] A total of eight selenium sites were identified (four per copy of MuSK-CRD) using data to 2.6 Å, with figure of merit (FOM) = 0.33 (Z-score = 33.5). Maximum likelihood density modification was performed with RESOLVE,[32] which yielded an interpretable electron density map into which three helices (from one copy of MuSK-CRD) were manually built. Because no non-crystallographic symmetry (NCS) was detected by SOLVE, molecular replacement (MOLREP[33]) was performed with the three-helix structure as a search model to place the second copy of MuSK-CRD in the asymmetric unit. NCS operators from MOLREP were then input to RESOLVE, and NCS averaging and phase-extension were performed to 2.4 Å, resulting in a dramatic improvement in the quality of the electron density map (FOM = 0.61). Autobuilding was performed in Arp/wArp[34], which successfully built 86 residues in copy A and 55 residues in copy B. Additional residues were built manually, and the partial model including 129 residues from copy A and 113 residues from copy B was refined against native data to 2.1 Å resolution. Model building was performed in Coot[35] and structure refinement in REFMAC.[36] The final model contains residues 314-454 in copy A (residues 313 and 455-494 are disordered) and residues 313-466 in copy B, excluding residues 457-461, which are disordered along with residues 467-494. Structure validation was performed with PROCHECK.[37]

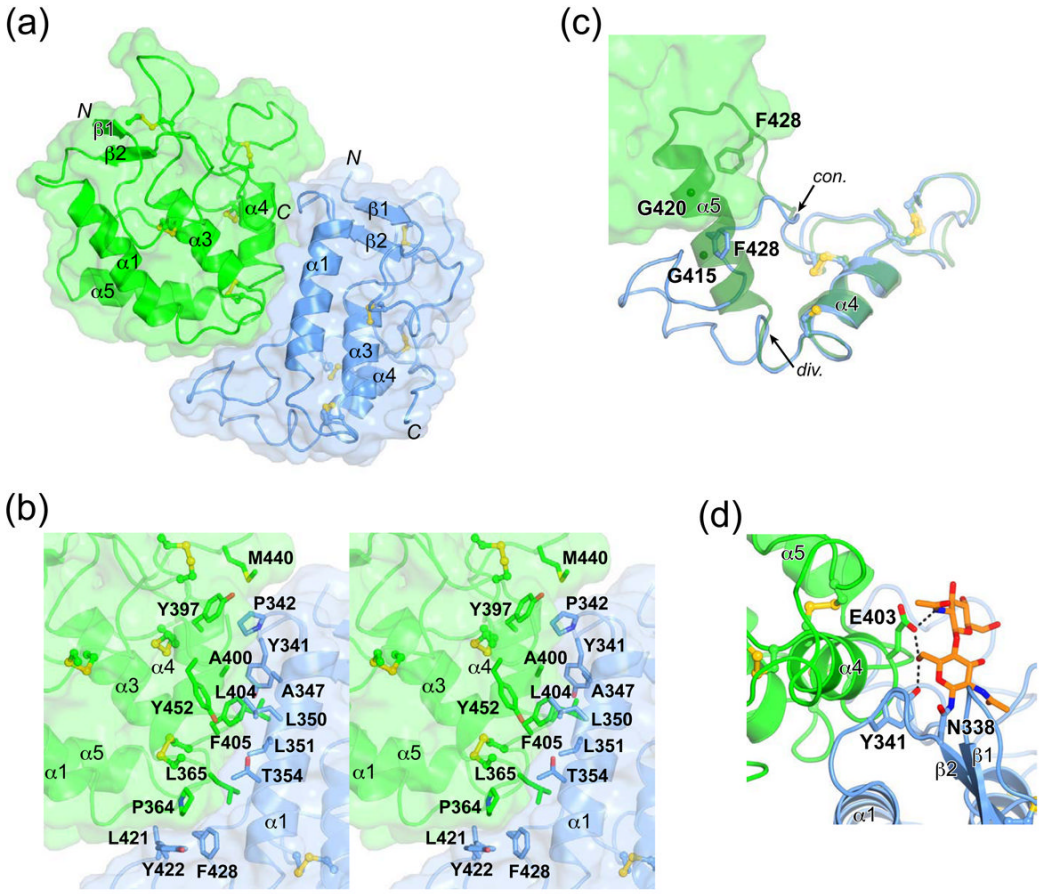

Figure 2.

Asymmetric dimer formation. (a) The two copies of MuSK-CRD in the asymmetric unit are colored green (copy A) and blue (copy B). The orientation for copy A is the same as in Figure 1(b). (b) Stereo view of the asymmetric dimer interface. Select interface residues are labeled. The orientation is the same as in (a). (c) Superposition of MuSK-CRD copy A (dark green) onto copy B (blue) to highlight the divergence in the C-terminal region of the two copies (arrows, divergence (*div.*) and convergence (*con.*)). Also note that the presence of α5 in copy B would be incompatible with formation of this asymmetric dimer. Same orientation as in (a). For clarity, only the C-terminal halves of copy B and superimposed copy A are shown. Copy A (original position) is shown in surface representation. The positions of the two glycines in α5 of superimposed copy A are indicated by small spheres at the Cα positions. (d) View of the Asn338 glycosylation site of MuSK-CRD in copy B (blue). Carbon atoms of the carbohydrate moiety are colored orange. Hydrogen bonds between the sugars and the protein are shown as dashed lines.

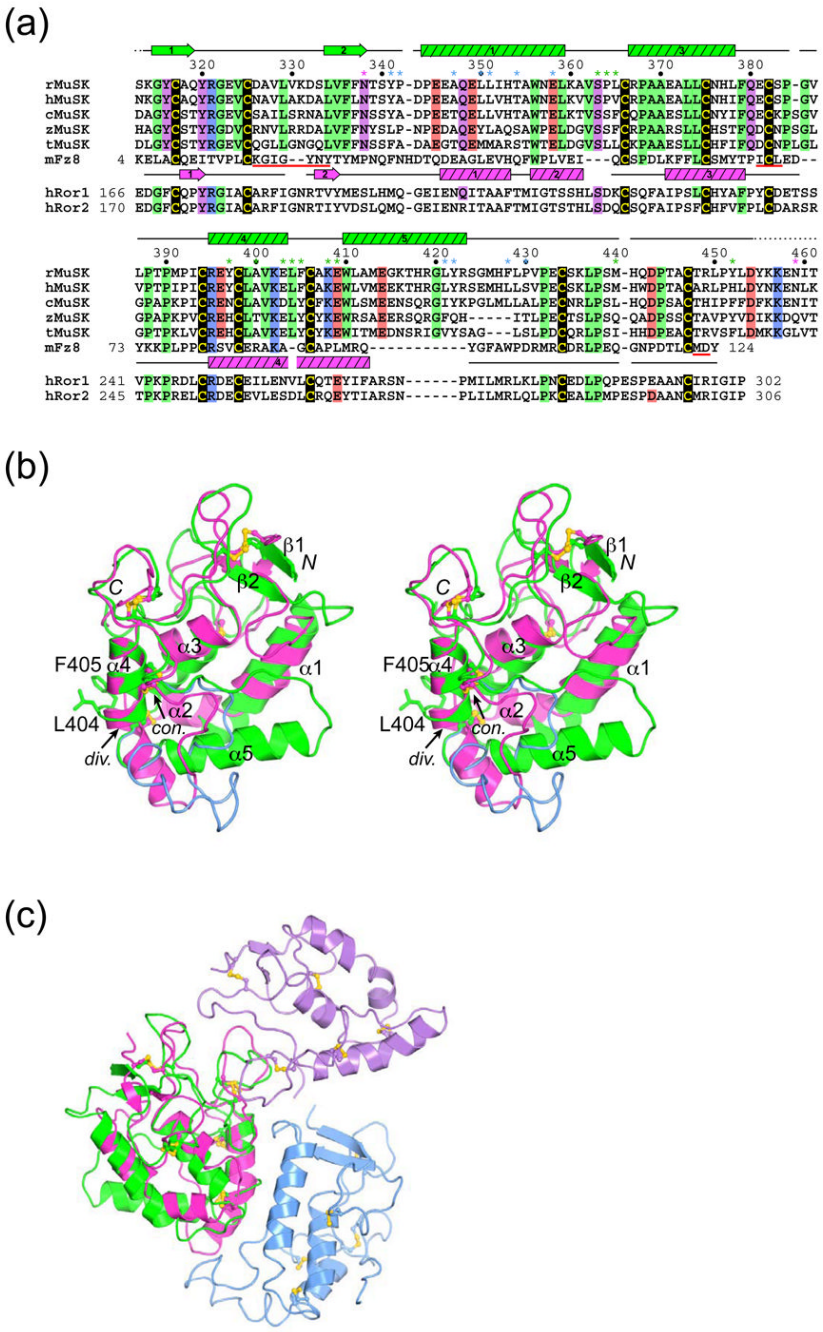

Figure 3.

Structural comparison of MuSK-CRD with other Fz-CRDs. (a) Structure-based sequence alignment of Fz-CRDs. The sequences of MuSK-CRD from rat, human, chick, zebrafish, and *Torpedo californica* are shown, along with the sequences from mouse Frizzled-8 (mFz8) and human Ror1 and Ror2. Residue numbering for rat MuSK appears above the rat sequence, and residue numbering for mFz8 (according to Dann et al.[19]) and hRor1/2 is in-line. As determined by PROCHECK,[37] secondary-structure elements for the MuSK-CRD structure appear above the MuSK sequences, and those for the mFz8-CRD structure (PDB code 1IJY)[19] appear below its sequence. A dashed line in the MuSK-CRD secondary structure indicates a disordered region. MuSK-CRD residues that are identical in the four species are boxed in the following

colors: black, cysteine residues; green, hydrophobic residues; purple, hydrophilic residues; red; acidic residues; and blue; basic residues. Those residues in mFz8 and hRor1/2 that match the conserved residues in the four MuSK species are also boxed. Residues that contribute to the asymmetric dimer interface are shown with an asterisk, either green for MuSK-CRD copy A or blue for copy B. The two N-linked glycosylation sites are indicated with a magenta asterisk. Regions in mFz8 that are important for Wnt binding (as revealed by alanine-scanning mutagenesis[19]) are shown underlined in red. (b) Stereo view of a superposition (10 cysteine Cα positions aligned) between MuSK-CRD (copy A) and mFz8-CRD (PDB code 1IJY),[19] in approximately the same orientation as in Figure 1(c). MuSK-CRD is colored green and mFz8-CRD is colored magenta. The side chains of Leu404 and Phe405 at the end of α4 are shown in stick representation. The divergent C-terminal region of copy B of MuSK-CRD (superimposed onto copy A), residues 406-434, is colored blue. The arrows indicate where in the C-terminal region the MuSK- and mFz8-CRD structures diverge (*div.*) and converge (*con.*). (c) Asymmetric MuSK-CRD dimer versus symmetric mFz8-CRD dimer. Copy A of MuSK-CRD (green) and mFz8-CRD (magenta) have been superimposed via their cysteine residues. Copy B of MuSK-CRD is colored blue (as before) and copy B of mFz8-CRD is colored purple. The orientation of MuSK-CRD (copies A and B) is the same as in Figure 2(a).

Table 1

X-Ray data collection and refinement statistics

Data collection	**SeMet**	**Native**
Resolution (Å)	50.0-2.3	50.0-2.1
Observations (>1σ)	120,809	58,852
Unique reflections	33,127	22,050
Completeness[a] (%)	97.6 (85.4)	97.6 (96.9)
R_{sym}[a,b] (%)	6.0 (24.0)	5.6 (29.0)
<I/σI>	9.0 (2.1)	16.8 (2.7)
Refinement		
Number of atoms		
Protein		2230
Carbohydrate		56
Water		63
Resolution (Å)		50.0-2.1
Reflections		20,869
R_{cryst}/R_{free}[c] (%)		22.6 / 26.4
rmsd values		
Bond lengths (Å)		0.007
Bond angles (°)		1.07
B-factors[d] (Å^2) (backbone / side chain)		0.43 / 0.80
Average *B*-factors (Å^2)		
All atoms		38.5
Protein		38.2
Carbohydrate		48.5
Water		38.0
Ramachandran plot statistics		
Most favored (%)		93.5
Additionally allowed (%)		6.5
Generously allowed (%)		0
Disallowed (%)		0

A PCR-amplified fragment of rat MuSK cDNA (residues 313-494) encoding MuSK-CRD and the extracellular juxtamembrane region was ligated into baculoviral transfer vector pAcGP67His-B (gift of Dr. Kermit Carraway, U.C.-Davis), and the sequence verified by automated DNA sequencing. This vector includes the secretion signal from the baculovirus envelope glycoprotein gp67 which is cleaved upon secretion, and an N-terminal His-tag. Recombinant baculovirus was generated by co-transfecting *Spodoptera frugiperda* (*Sf*9) cells with the pAcGP67HisB-Fz-CRD vector and linearized Baculogold DNA (BD Biosciences). For large-scale protein production, high-titer baculovirus was used to infect *Sf*9 cells in suspension culture at a density of 1-2 × 10^6 cells/ml. Cell medium containing the secreted MuSK-CRD was harvested 72 h post-infection by centrifugation and sterile-filtered through 0.22 μm filters. MuSK-CRD was purified by nickel-affinity chromatography (Ni-NTA; Qiagen), gel-filtration chromatography (Superdex 75, GE Healthcare), and anion-exchange chromatography (Source Q, GE Healthcare).

The protocol for selenomethionine labeling was derived from Bellizzi et al.[32] *Sf*9 cells were grown in suspension in EX-CELL 420 medium to a density of 2 × 10^6 cells/ml and infected with MuSK-CRD baculovirus. 24 h post-infection, the cells were harvested by centrifugation at 700 rpm for 10 min, the medium discarded, and cells washed in EX-CELL 421 medium lacking L-methionine (Sigma Aldrich) to remove traces of methionine-containing medium. Cells were then incubated for 4-6 h in EX-CELL 421 medium to deplete the cellular pool of L-methionine. After this depletion period, the cells were harvested by centrifugation, and resuspended in L-methionine-deficient EX-CELL 421 medium supplemented with 50 mg/L L-selenomethionine (ACROS). Cells were maintained in labeling medium for an additional 48 hr, at which time MuSK-CRD-containing medium was collected, and protein

purified as described above. The efficiency of selenomethionine incorporation was determined by MALDI-TOF analysis of trypsinized MuSK-CRD. In two independent experiments, selenomethionine labeling occurred at 55 and 60% efficiency.

Crystals of wild-type, glycosylated MuSK-CRD at 10-15 mg/ml were obtained at 22°C in hanging drops (1:1 v:v ratio) with reservoir buffer containing 25-30% polyethylene glycol 4000, 0.1 M Tris, pH 8.5, 0.2 M sodium acetate, and 3-5% glycerol. Crystals belong to space group $P2_1$ with unit cell dimensions of a=65.59 Å, b=44.42 Å, c=69.53 Å, ⟨=©=90°, and ®=108.27°. There are two MuSK-CRD molecules in the asymmetric unit with a solvent content of approximately 44%. Prior to stream freezing in liquid nitrogen, crystals were equilibrated in a series of cryosolvents containing 10%, 15%, and 20% glycerol. A 2.1 Å native dataset was collected at beamline X4A, National Synchrotron Light Source, Brookhaven National Laboratory, and a 2.3 Å dataset from a single selenomethionyl-substituted crystal was collected on beamline X4C at λ=0.9787 Å, just above the selenium absorption peak. Image indexing, integration and scaling were performed using HKL2000[33].

a The overall value is given first, with the value in the highest resolution shell (2.38-2.30 Å or 2.18-2.10 Å) given in parenthesis.

b $R_{sym} = 100 \times \Sigma|I - \langle I \rangle|/\Sigma I$.

c $R_{cryst} = 100 \times \Sigma||F_O| - |F_C||/\Sigma|F_O|$, where F_O and F_C are the observed and calculated structure factors, respectively ($F_O > 0\ \sigma$). R_{free} was determined from ~5% of the data (1129 reflections).

d For bonded atoms.